*Article*

# Evaluation of Petroleum Hydrocarbon-Contaminated Soil Remediation Technologies and Their Effects on Soybean Growth

**Dengyu Jiang [1,†], Tao Li [2,†], Xuanhe Liang [2], Xin Zhao [2], Shanlong Li [2], Yutong Li [1], Kokyo Oh [3], Haifeng Liu [1,*] and Tiehua Cao [2,\*]**

1    College of Agriculture, Yanbian University, Yanji 133002, China; a1940590572@163.com (D.J.); lyutong233@126.com (Y.L.)
2    Institute of Agricultural Resources and Environments, Jilin Academy of Agricultural Sciences (Northeast Agricultural Research Center of China), Changchun 130033, China; ndlitao@126.com (T.L.); liangxuanhe_2004@163.com (X.L.); zhaoxin8401@163.com (X.Z.); lishanlong05@163.com (S.L.)
3    Center for Environmental Science in Saitama, Saitama 347-0115, Japan; o.kokyo@pref.saitama.lg.jp
*    Correspondence: lhf@ybu.edu.cn (H.L.); caotiehua2002@163.com (T.C.)
†    These authors contributed equally to this work.

**Abstract:** The application of persulfate (PS) for the remediation of petroleum hydrocarbon contamination is among the most widely employed in situ chemical oxidation (ISCO) techniques, and it has received widespread attention due to its limited impact on soil integrity. This study employed a $FeSO_4$-activated PS oxidation method to investigate the feasibility of remediating soil contaminated with total petroleum hydrocarbons (TPHs). The factors tested included the TPH concentration, different $PS:FeSO_4$ ratios, the reaction time for remediation, soil physical and chemical property changes before and after remediation, and the effect of soil before and after remediation on soybean growth. The TPH degradation rate in soil was highest for high-, medium-, and low-TPHs soils—81.5%, 81.4%, and 72.9%, respectively, with minimal disruption to the soil's physicochemical properties—when $PS:FeSO_4 = 1:1$. The remediation verification results indicated that the condition of the soybeans was optimal when $PS:FeSO_4 = 1:1$. Under this condition, the net photosynthetic rate, stomatal conductance, intercellular $CO_2$ concentration, and transpiration rate all remained high. Therefore, the best remediation effect was achieved with $PS:FeSO_4 = 1:1$, which also minimized the damage to the soil and the effects on crop growth.

**Keywords:** chemical oxidation; petroleum-contaminated soil; sodium persulfate; soybeans

## 1. Introduction

The increasing production and consumption of oil have led to significant contamination of soils during extraction, transportation, and processing, resulting in oil pollution becoming a growing global concern [1]. Total petroleum hydrocarbons (TPHs), which include alkanes, polycyclic aromatic hydrocarbons (PAHs), and olefins, are toxic, carcinogenic, and difficult to remove once adsorbed onto soil particles [2]. Given the severity of this form of pollution, extensive research has been conducted to develop methods for removing TPHs from contaminated soils. Among these methods, chemical oxidation has emerged as an effective remediation technique [3].

In situ chemical oxidation (ISCO) is gaining popularity due to its flexibility across different types of contaminated sites. Among the three common ISCO methods—catalyzed ($H_2O_2$) propagation, permanganate, and activated persulfate (PS)—the activated PS method has emerged as the most widely used in field applications [4]. For soils with high contaminant concentrations, the first two oxidants require high doses, which increases costs

and can impact soil properties and harm microbial communities [5]. In contrast, when activated, PS produces sulfate radicals ($SO_4^-$) with a high redox potential ($E_0$ = 2.5–3.1 V), capable of degrading most organic pollutants [6,7]. Under activation methods involving heat, UV light, transition metals, carbon-based materials, or $H_2O_2$, stronger oxidants such as $\cdot SO_4$ ($E_0$ = 2.4 V) and hydroxyl radicals (OH, $E_0$ = 2.8 V) are generated, further enhancing degradation [8–11]. $Fe^{2+}$-activated persulfate is the most frequently studied for the in situ remediation of hydrocarbon-contaminated soils because of its high efficiency, environmental friendliness, and long-term stability, and $Fe^{3+}/Fe^{2+}$ could stimulate microbial activity [12]. However, there have been few studies using in situ PS oxidation to treat long-term, complex TPH-contaminated soils [13].

This study conducted batch experiments to remediate TPH-contaminated soil using various ratios of $FeSO_4$ and PS. We assessed TPH degradation rates, changes in crude oil components, soil pH, and electrical conductivity during the remediation process. Post-remediation, a phytoremediation experiment was performed to measure the plant height, leaf nitrogen content, chlorophyll content, net photosynthetic rate, and respiration rate of soybeans under different treatment conditions [14]. The objectives were to

(1)  Evaluate the impact of different $FeSO_4$ and PS ratios on TPH removal.
(2)  Investigate the effects of PS remediation on soil physicochemical properties in TPH-contaminated soil.
(3)  Assess the suitability of various $FeSO_4$ and PS treatments for crop growth.

## 2. Materials and Methods

### 2.1. Soil Samples and Chemicals Used in the Study

Analytical-grade ferrous sulfate heptahydrate ($FeSO_4 \cdot 7H_2O$) was obtained from Tianjin Damao Chemical Reagent Factory (China), and sodium persulfate ($Na_2S_2O_8$) was sourced from Shanghai Macklin Biochemical Co., Ltd. (Shanghai, China). Ultrapure water was used for all experiments.

Soil samples for the experiments were collected from farmland near an oil well in Songyuan City, Jilin Province, China (45°10′ N, 124°48′ E). The topsoil samples were collected at distances of 50 m, 500 m, and 1000 m from the pollution source, at a depth of 30 cm at each sampling point. The samples were stored in brown glass bottles with PTFE-sealed caps, refrigerated, and transported to the laboratory to maintain moisture levels. The soil was thoroughly mixed in the laboratory, sieved through a 2 mm mesh, and analyzed to determine the TPH concentration. The TPH concentrations of the contaminated soil were measured as follows: at 50 m from the pollution source, the TPH concentration was greater than 18,000 mg/kg; at 500 m, the TPH concentration ranged from 12,000 to 18,000 mg/kg; and at 1000 m, the TPH concentration was less than 12,000 mg/kg. The collected soils were then mixed according to their distances from the pollution source, and their TPH concentrations were measured. Based on the TPH concentrations, the soils were classified into three pollution levels: high concentration (19,070 ± 477.3 mg/kg) at 50 m from the pollution source, medium concentration (14,792 ± 350.5 mg/kg) at 500 m, and low concentration (10,801 ± 200.9 mg/kg) at 1000 m. The physical and chemical properties and content of the petroleum hydrocarbon fractional components of the soil are listed in Table 1.

**Table 1.** Physical and chemical properties of high, medium, and low TPH concentration contaminated samples.

| Characteristics | Analysis | Soil |
|---|---|---|
| High-concentration petroleum hydrocarbon-contaminated soil | Total N(g/kg) | $95.58 \pm 5.3$ |
| | Total P(g/kg) | $1.392 \pm 0.01$ |
| | Total K(g/kg) | $3.23 \pm 0.03$ |
| | SOM (g/kg) | $30.7 \pm 0.1$ |
| | pH | $6.84 \pm 0.05$ |
| | Electrical conductivity | $7.3 \pm 0.05$ |
| | C10–C17(mg/kg) | $10{,}247 \pm 323.6$ |
| | C18–C30(mg/kg) | $7232 \pm 123.3$ |
| | C31–C40(mg/kg) | $1591 \pm 15.3$ |
| | Total(mg/kg) | $19{,}070 \pm 477.3$ |
| Medium-concentration petroleum hydrocarbon-contaminated soil | Total N(g/kg) | $91.12 \pm 5.3$ |
| | Total P(g/kg) | $1.389 \pm 0.01$ |
| | Total K(g/kg) | $3.22 \pm 0.01$ |
| | SOM(g/kg) | $33.9 \pm 0.1$ |
| | pH | $6.62 \pm 0.05$ |
| | Electrical conductivity | $8.9 \pm 0.05$ |
| | C10–C17(mg/kg) | $6886 \pm 100.3$ |
| | C18–C30(mg/kg) | $7906 \pm 116.5$ |
| | C31–C40(mg/kg) | $701 \pm 7.1$ |
| | Total(mg/kg) | $14{,}792 \pm 350.5$ |
| Low-concentration petroleum hydrocarbon-contaminated soil | Total N(g/kg) | $85.31 \pm 4.6$ |
| | Total P(g/kg) | $1.396 \pm 0.01$ |
| | Total K (g/kg) | $3.21 \pm 0.01$ |
| | SOM (g/kg) | $32.8 \pm 0.1$ |
| | pH | $6.59 \pm 0.04$ |
| | Electrical conductivity | $9.4 \pm 0.05$ |
| | C10–C17(mg/kg) | $6749 \pm 98.5$ |
| | C18–C30(mg/kg) | $4052 \pm 90.5$ |
| | C31–C40(mg/kg) | $287 \pm 5.6$ |
| | Total(mg/kg) | $10{,}801 \pm 200.9$ |

The values are the means $\pm$ SD. SOM = soil organic matter.

## 2.2. Experimental Design

The remediation experiments were conducted in two phases and were prepared in 42 plastic drums (top diameter 25.0 cm, bottom diameter 19.8 cm, and height 29.3 cm) with capacities of 15 L. Each treatment was performed in triplicate. The experiment was set up in a closed, light-proof laboratory at the Jilin Academy of Agricultural Sciences in China, and the specific process was as follows.

Chemical oxidation stage: 75 g of PS were dissolved in 1 L of deionized water, added to 5 kg of contaminated soil (high, medium, and low TPHs) in a plastic bucket with a capacity of 15 L, and continuously stirred for 5 min. The test soil was then treated with 69.6 g (TA1, TB1, TC1), 87.0 g (TA2, TB2, TC2), 104.4 g (TA3, TB3, TC3), and 121.81 g (TA4, TB4, TC4) (FeSO$_4$·7H$_2$O) for PS activation. Additionally, high, medium, and low petroleum hydrocarbon-contaminated soils natural oxidation treatment (CK1, CK2, CK3). All experimental procedures were conducted at room temperature, with soil moisture maintained at $25-35\%$ (soil moisture content was measured daily using the Decagon Devices–HydroSense II from METER Group (Pullman, WA, USA), and water was sprayed as needed to maintain the soil moisture level. Soil samples were collected on the 3rd, 7th, and 14th days, stored in brown glass bottles with PTFE-sealed caps, and the TPH

concentrations and their components were measured promptly. On the 14th day, the physicochemical properties of the soil were also measured.

Crop restoration verification stage: soybeans (variety: [Heihe 43 in China]) were planted in the soil 14 days after PS oxidation. Leaf measurements were taken at the flowering stage (Day 50) and pod-setting stage (Day 72) to assess the net photosynthetic rate, stomatal conductance, intercellular $CO_2$ concentration, and transpiration rate [15].

*2.3. The TPH Concentration and Fraction Analysis*

The TPH concentration in the soil was determined using the gas chromatography method specified in the "Soil and Sediment Petroleum Hydrocarbons (C10−C40) Determination" by the Ministry of Ecology and Environment of the People's Republic of China (HJ1021-2019). Samples were collected on days 10, 14, 21, 24, 28, and 35. During soil sampling, the plastic bucket contents were thoroughly mixed before soil collection using the five-point sampling method. The sampling points were centered at the center of the bucket, and four additional sampling points were selected at the intersections of two perpendicular diameters along the circumference of the bucket, with 2.5 g of soil collected from each point. The collected soil was then re-mixed to ensure uniformity and eliminate any potential biases. After removing debris, approximately 10 g of each sample (accurate to 0.01 g) was weighed, mixed with an appropriate amount of anhydrous sodium sulfate, sealed, and stored in the dark at temperatures below 4 °C for subsequent analysis. All samples were tested in duplicate.

Soil samples were extracted using a 1:1 mixture of n-hexane and acetone for 16 to 18 h, with the reflux rate controlled at 8−10 cycles per hour. After cooling, the extracts were concentrated and purified. The TPHs in the solvent extracts were analyzed using a GC-2010 gas chromatograph (Himadzu Corporation, Kyoto, Japan) equipped with a quartz capillary column (30 mm × 0.32 mm × 0.25 μm) with a stationary phase of 5% phenyl-95% methylpolysiloxane. Gas flow rates were set to 15 mL/min for high-purity nitrogen, 30 mL/min for hydrogen, and 300 mL/min for air, with the flame ionization detector set to 325 °C. A 1 μL sample was injected, and the temperature program was set as follows: an initial increase from 50 to 230 °C at 40 °C/min, followed by an increase from 230 to 320 °C at 20 °C/min, and held at 320 °C for 9 min [16]. The total run time was 20 min. The TPH degradation rate was calculated with a kinetic equation as follows:

$$RE = (C_0 − C_t)/C_0 \times 100\% \qquad (1)$$

where RE is the TPHs removal rate, and ($C_t$) and ($C_0$) are the TPH concentrations at time t and zero, mg/kg, respectively [17].

*2.4. Soil Properties Analysis*

Soil pH was measured with a PHS-3C pH (Shanghai Instrument Electric Scientific Instrument Co., Ltd., Shanghai, China) meter using the potentiometric method. Electrical conductivity was assessed with a DDS-307 (Shanghai Instrument Electric Scientific Instrument Co., Ltd., Shanghai, China) conductivity meter, adhering to the electrode method for soil conductivity determination. Total nitrogen, phosphorus, and potassium in the soil were analyzed using standard elemental analysis methods for agricultural land in China.

*2.5. Crop Growth Physiological Traits*

During the flowering and pod-setting stages, three representative soybean plants with uniform growth were selected between 9:00 and 11:30 on clear days. The photosynthetic parameters of fully expanded top leaves were measured using the Li-6400 portable gas exchange system (Li-COR, Lincoln, NE, USA). For all treatments, photosynthetic active radiation (PAR) was set to 1500 $\mu mol \cdot m^{-2} \cdot s^{-1}$, with a flow rate of 500 $\mu mol \cdot s^{-1}$. The leaf chamber temperature was adjusted based on gas chamber conditions, and the reference chamber $CO_2$ concentration was set to the outdoor $CO_2$ concentration plus 200 $\mu mol \cdot mol^{-1}$. After the system stabilized (20–30 min), fully expanded top leaves were selected to measure the photosynthetic rate, stomatal conductance, intercellular $CO_2$ concentration, and transpiration rate [15,18].

*2.6. Statistical Analysis*

All analyses were performed in triplicate. The results were expressed as the average of three independent measurements. The photosynthetic rate, stomatal conductance, intercellular $CO_2$ concentration, and transpiration rate [15,18] were analyzed using SPSS version 27.0. An ANOVA was applied to determine the statistical significance of mean values ($n = 3$) at $p \leq 0.05$. All statistical characteristics and data were analyzed using Origin 2021 (OriginLab Corporation, Northampton, MA, USA) and SPSS (IBM corporation, Armonk, NY, USA). A bioinformatic analysis was performed using the OmicStudio tools at https://www.omicstudio.cn/tool on 4 November 2024.

# 3. Results and Discussion

## 3.1. The Degradation of TPHs and Fraction Analysis

Figures 1–3 show the changes in TPH concentrations in soils with different contamination levels 14 days after oxidation with different $PS:FeSO_4$ ratios. The residual TPH concentration was lowest in high-, medium-, and low-TPH soils when $PS:FeSO_4$ = 1:1. The initial TPH concentrations were 19,070 ± 477.3 mg/kg in high-TPH soil, 14,792 ± 350.5 mg/kg in medium-TPH soil, and 10,801 ± 200.9 mg/kg in low-TPH soil. After 3 days, in high-TPH soil, the TPH concentration was 6330 ± 103.2 mg/kg; in medium-TPH soil, the TPH concentration was 4415 ± 96.3 mg/kg; and in low-TPH soil, the TPH concentration was 4244 ± 100.3 mg/kg. After 7 days, in high-TPH soil, the TPH concentration was 5180 ± 88.7 mg/kg; in medium-TPH soil the TPH concentration was 3554 ± 100.3 mg/kg; and in low-TPH soil, the TPH concentration was 3215 ± 65.3 mg/kg. After 14 days, the lowest TPH concentrations were 4144 ± 220.2 mg/kg in high-TPH soil, 2877 ± 138.0 mg/kg in medium-TPH soil, and 2894 ± 121.8 mg/kg in low-TPH soil. Under natural oxidation conditions, the TPH concentrations in the soils changed over time. After 3 days, the concentrations were as follows: high-TPH soil, 14,912 ± 200.3 mg/kg; medium-TPH soil, 11,611 ± 193.6 mg/kg; and low-TPH soil, 8673 ± 113.2 mg/kg. After 7 days, the concentrations were as follows: high-TPH soil, 14,798 ± 193.6 mg/kg; medium-TPH soil, 11,522 ± 168.3 mg/kg; and low-TPH soil, 8554 ± 126.3 mg/kg. After 14 days, the concentrations were as follows: high-TPH soil, 14,645 ± 210.2 mg/kg; medium-TPH soil, 11,449 ± 156.3 mg/kg; and low-TPH soil, 8551 ± 96.3 mg/kg. This indicates that $FeSO_4$-activated PS oxidation can rapidly reduce the TPH concentration in petroleum hydrocarbon-contaminated soil. Over time, however, the TPH degradation rate significantly decreases [19,20]. This may be because as the petroleum hydrocarbons in the soil are gradually degraded, they are less likely to adhere to $\cdot SO_{4-}$ and $\cdot OH$ radicals, which leads to a slower rate of decrease in the residual TPH concentration. A similar trend was also found in a previous study of the chemical oxidation of TPH-contaminated soil using PS [21]. The study found that when using PS chemical oxidation in combination with

bioremediation to treat TPH-contaminated soil, after 12 days of remediation, the TPHs concentration decreased from 16,622.81 to 7848.80 mg/kg, and, by the 60th day, the TPH concentration was 2815.77 mg/kg [8].
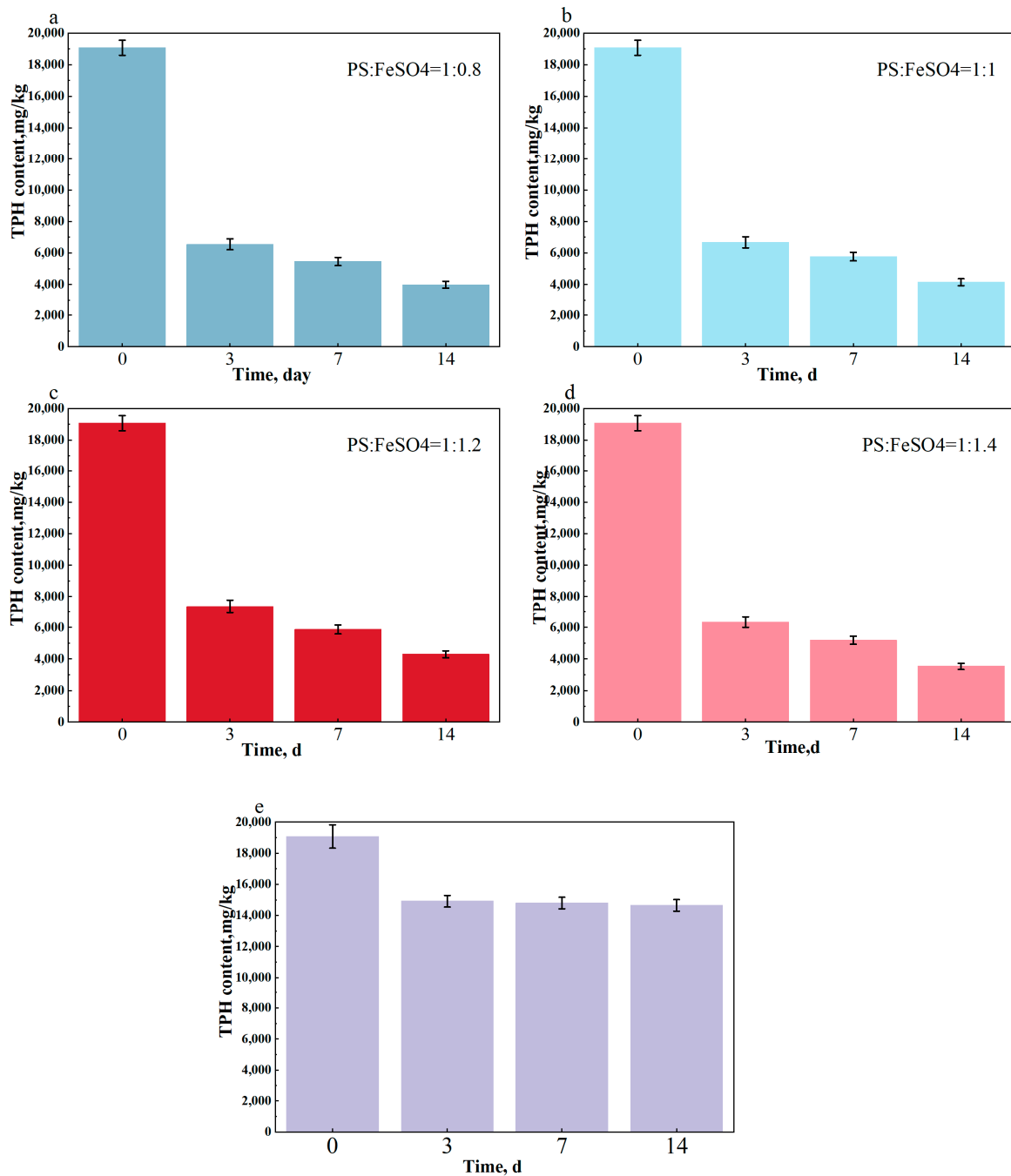


**Figure 1.** Changes in soil TPH concentrations with PS oxidation remediation over 14 d: (**a**) PS:FeSO$_4$ = 1:0.8; (**b**) PS:FeSO$_4$ = 1:1; (**c**) PS:FeSO$_4$ = 1:1.2; (**d**) PS:FeSO$_4$ = 1:1.4; (**e**) natural conditions oxidation (contrast). Experimental conditions: initial TPH concentration = 19,070 ± 477.3 mg/kg; pH = 6.84.
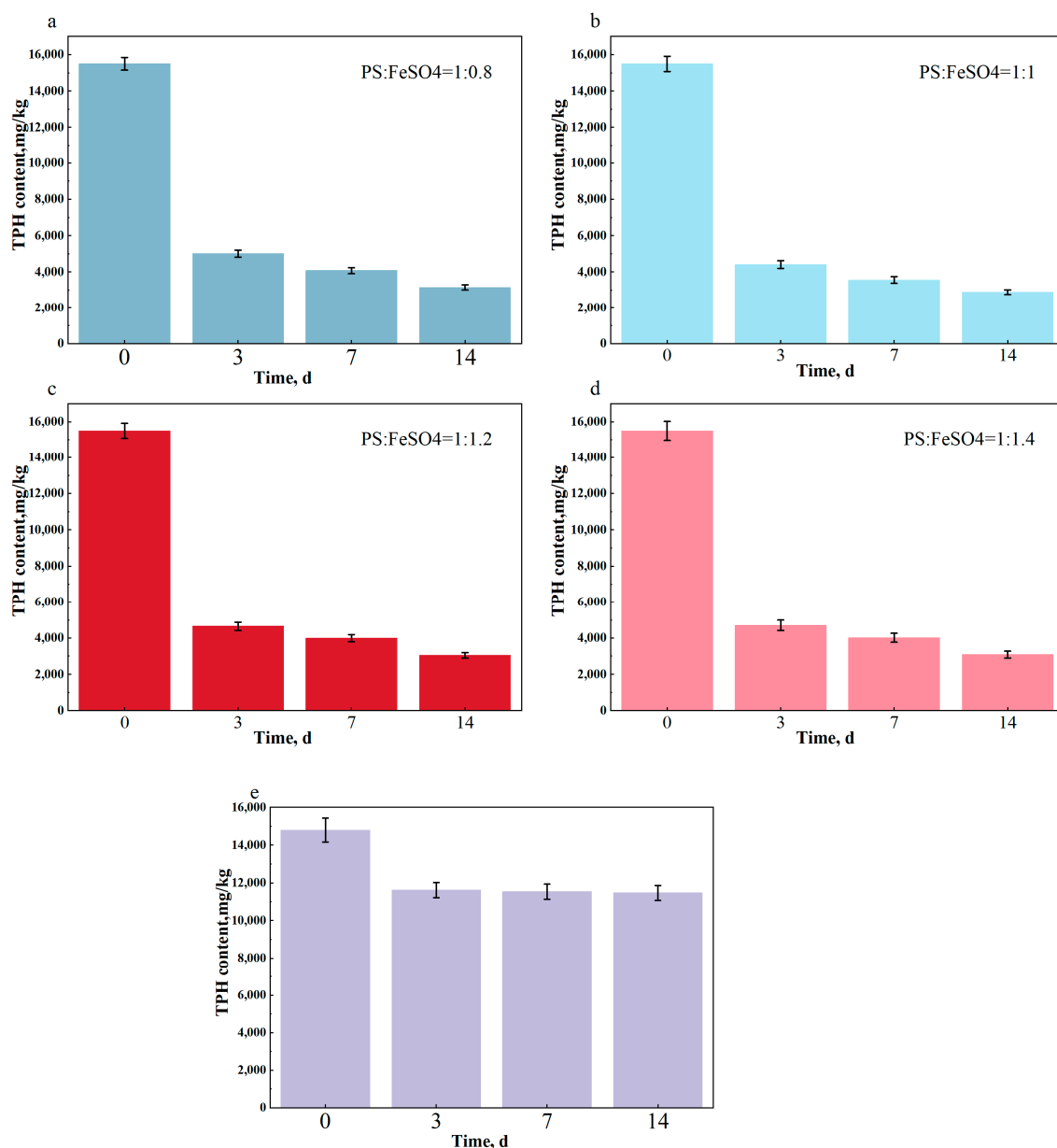
**Figure 2.** Changes in soil TPH concentrations with PS oxidation remediation over 14 d: (**a**) PS:FeSO$_4$ = 1:0.8; (**b**) PS:FeSO$_4$ = 1:1; (**c**) PS:FeSO$_4$ = 1:1.2; (**d**) PS:FeSO$_4$ = 1:1.4; (**e**) natural conditions oxidation (contrast). Experimental conditions: initial TPH concentration = 14,792 ± 350.5 mg/kg; pH = 6.62.

Figures 4–6 show the changes in the proportions of TPH components with different carbon chain lengths in soils with varying contamination levels 14 days after oxidation, using four different PS:FeSO$_4$ ratios. In high-TPH soil, the proportion of C18–C30 components decreased from 37.9% to 33.2%, 30.8%, 31.7%, 32.0%, and 36.2% for PS:FeSO$_4$ ratios of 1:0.8, 1:0.9, 1:1, 1:1.2, and natural conditions oxidation, respectively. The proportion of C11–C17 components decreased from 53.7% to 49.7%, 50.3%, 50.3%, 50.4%, and 52.2%, and the proportion of C31–C40 components increased from 8.3% to 17.1%, 18.9%, 17.9%, 17.5%, and 11.5%, respectively. In medium-TPH soil, the proportion of C11–C17 components decreased from 44.4% to 40.3%, 41.2%, 40.4%, 40.4%, and 42.2%, respectively. There were no significant changes in the C18–C30 components, while the proportion of C31–C40 components increased from 4.5% to 8.8%, 7.6%, 8.0%, and 8.3%, respectively. In low-TPH soil, C11–C17 decreased from 60.8% to 41.3%, 41.5%, 41.9%, 41.4%, and 60.4%. The proportion of C18–C30

components increased from 36.5% to 53.0%, 52.9%, 52.6%, 52.9%, and 35.1%. The treatments showed no significant differences, with no significant changes in C18–C30 components, while the proportion of C31–C40 components increased from 2.7% to 5.7%, 5.6%, 5.5%, 5.7%, and 4.5%. Across all contamination levels, the proportion of long-chain molecules increased, while the proportion of medium- and short-chain molecules decreased, with the latter showing a more significant reduction. This was likely due to the more stable structure of long-chain molecules, which are harder to oxidize, whereas short-chain molecules are less stable and more readily oxidized [22]. In a previous study, a similar trend was observed in the recalcitrance of C17−C40 oxidation after PS oxidation. The study found that most of the residual TPHs in the soil were C16−C44, including recalcitrant esters such as alkyl nitrates, chlorinated alkyl esters, and long-chain esters, as well as resistant aromatics, such as phthalate esters and benzoates that were activated by ultrasonication and heating [23].
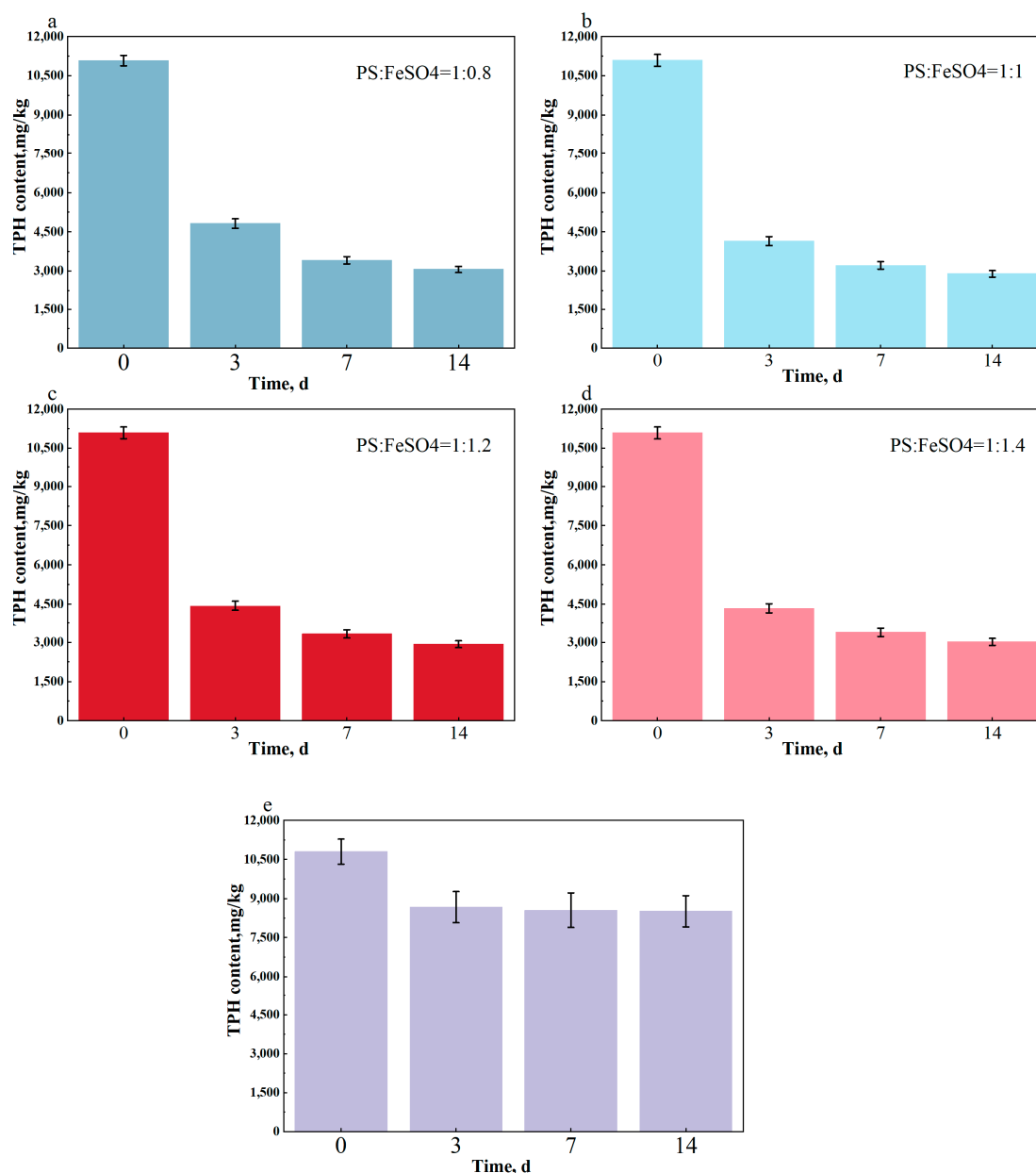


**Figure 3.** Changes in soil TPH concentrations with PS oxidation remediation over 14 d: (**a**) PS:FeSO$_4$ = 1:0.8; (**b**) PS:FeSO$_4$ = 1:1; (**c**) PS:FeSO$_4$ = 1:1.2; (**d**) PS:FeSO$_4$ = 1:1.4; (**e**) natural conditions oxidation (contrast). Experimental conditions: initial TPH concentration = 10,801 ± 200.9 mg/kg, pH = 6.59.
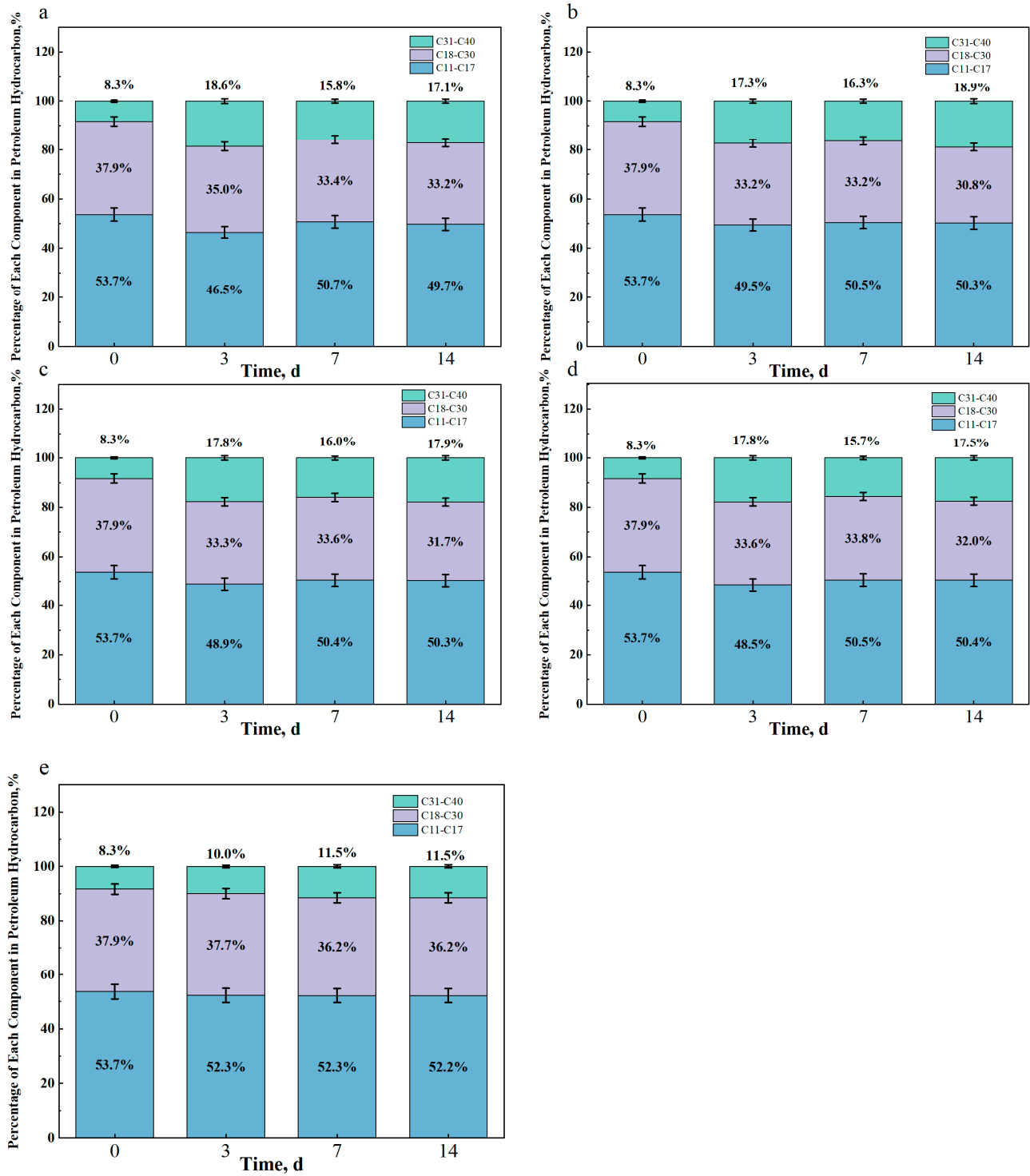
**Figure 4.** Changes in soil TPH concentrations with PS oxidation remediation over 14 d: (**a**) PS:FeSO₄ = 1:0.8; (**b**) PS:FeSO₄ = 1:1; (**c**) PS:FeSO₄ = 1:1.2; (**d**) PS:FeSO₄ = 1:1.4; (**e**) natural conditions oxidation (contrast). Experimental conditions: Initial TPH concentration = 19,070 ± 477.3 mg/kg; pH = 6.84.
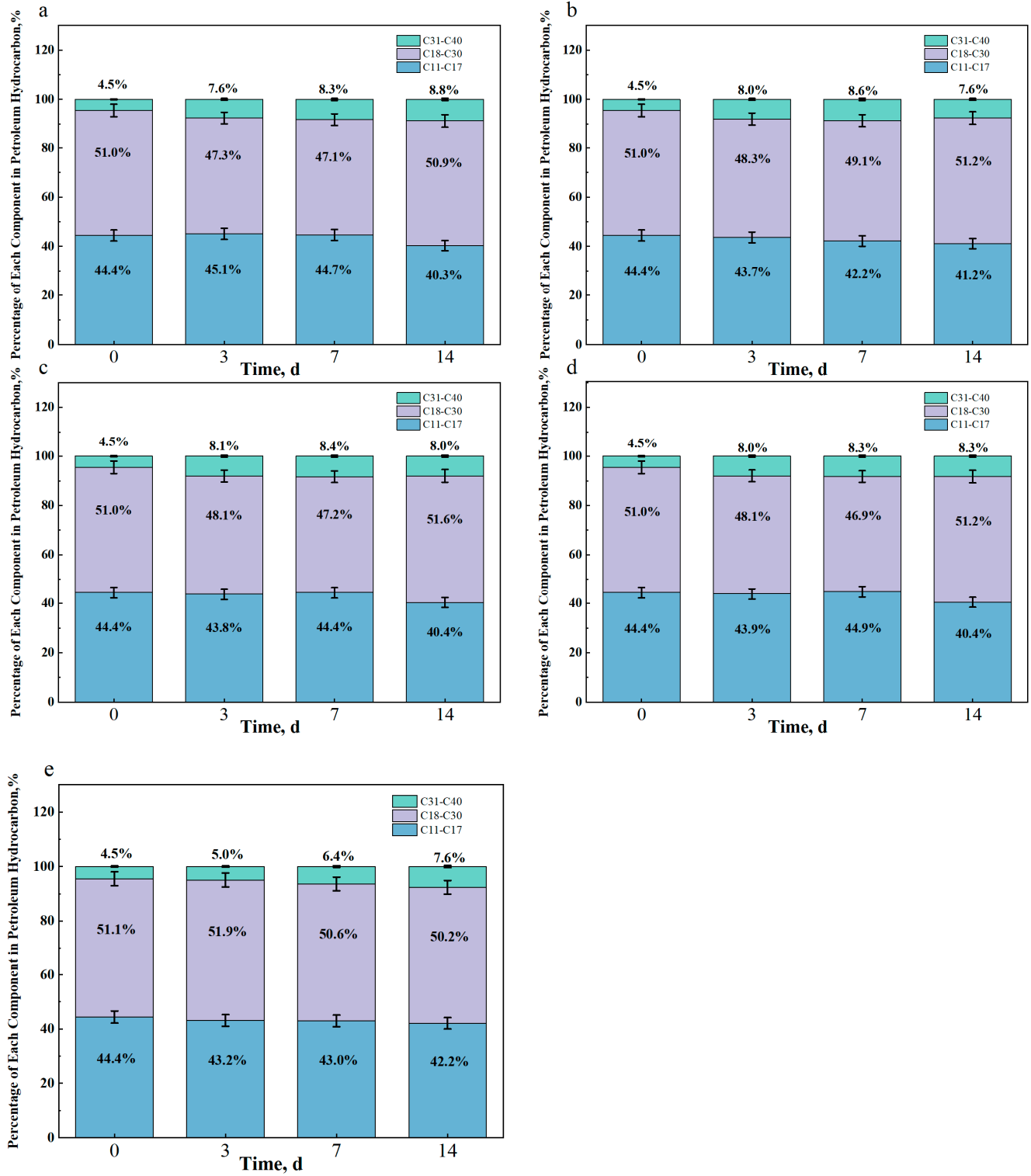
**Figure 5.** Changes in soil TPH concentrations with PS oxidation remediation over 14 d: (**a**) PS:FeSO$_4$ = 1:0.8; (**b**) PS:FeSO$_4$ = 1:1; (**c**) PS:FeSO$_4$ = 1:1.2; (**d**) PS:FeSO$_4$ = 1:1.4; (**e**) natural conditions oxidation (contrast). Experimental conditions: Initial TPHs = 14, 792 ± 350.5 mg/kg; pH = 6.62.
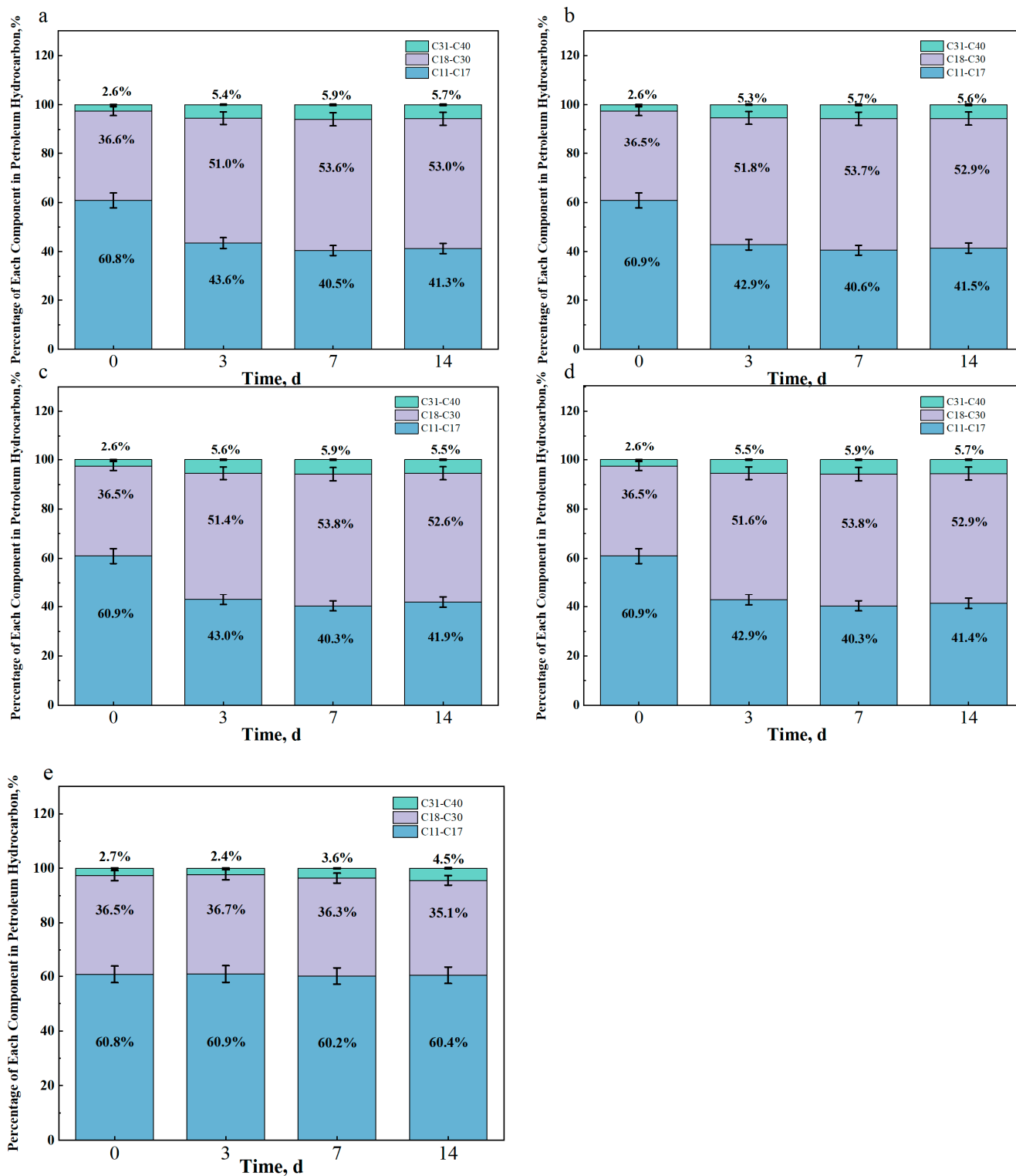
**Figure 6.** Changes in soil TPH concentrations with PS oxidation remediation over 14 d:
(**a**) PS:FeSO$_4$ = 1:0.8; (**b**) PS:FeSO$_4$ = 1:1; (**c**) PS:FeSO$_4$ = 1:1.2; (**d**) PS:FeSO$_4$ = 1:1.4; (**e**) natural conditions oxidation (contrast). Experimental conditions: Initial TPH concentration = 10,801 ± 200.9 mg/kg, pH = 6.59.

## 3.2. The Effect of Remediation on TPH Concentrations Under Different PS:FeSO$_4$ Ratios

The TPH degradation rates in soils with different initial contamination levels, 14 days after oxidation with varying PS:FeSO$_4$ ratios, are shown in Figure 7. In high-TPH soil, the degradation rates on day 3 were 61.4%, 66.8%, 65.6%, and 64.9% for PS:FeSO$_4$ ratios of

1:0.8, 1:0.9, 1:1, and 1:1.2, respectively. In medium-TPH soil, the degradation rates were 67.6%, 71.5%, 70.0%, and 69.6%, respectively, and in low-TPH soil, the degradation rates were 56.5%, 62.6%, 60.1%, and 61.0%, respectively. On day 7, TPH removal rates were 69.2%, 72.8%, 71.3%, and 69.7%, respectively, in high-TPH soil; 73.7%, 77.0%, 74.2%, and 74.1%, respectively, in medium-TPH soil; and 69.2%, 71.0%, 70.0%, and 79.4%, respectively, in low-TPH soil. These results suggest that by day 3, $SO_4^-$ had oxidized most of the TPH pollutants. Over time, the degradation rate of TPHs decreased. This was likely due to the oxidation of most short-chain TPH molecules, leaving behind the more resistant long-chain molecules. On day 14, the TPH removal rates were 77.4%, 81.5%, 79.1%, and 78.2%, respectively, in high-TPH soil; 79.7%, 81.4%, 80.3%, and 80.1%, respectively, in medium-TPH soil; and 72.4%, 72.9%, 73.5%, and 72.7%, respectively, in low-TPH soil. The removal rates were higher in high- and medium-TPH soils compared to low-TPH soils. This difference may be due to the lower pollutant concentrations in low-TPH soil, resulting in less contact between $SO_4^-$ from FeSO$_4$-activated PS and TPH pollutants [24,25]. The highest TPH removal rate was achieved with a 1:1 PS:FeSO$_4$ ratio, indicating that FeSO$_4$-activated PS effectively degraded most of the pollutants. As the FeSO$_4$ content increased, more activated $\cdot SO_4^-$ was generated, improving the degradation rate [26,27]. However, a further increase in FeSO$_4$ content resulted in a decrease in the degradation rate, which may have occurred due to excess $Fe^{2+}$ causing fluorescence quenching of $\cdot SO_{4-}$ through the following reaction: (1) $Fe^{2+}$ (aq) + $S_2O_8^{2-}$ (aq) $\rightarrow$ $Fe^{3+}$(aq)+$\cdot SO_4^-$ (aq) + $SO_4^{2-}$ (aq), (2) $Fe^{3+}$ (aq) + $S_2O_8^{\ 2-}$ (aq) $\rightarrow$ $Fe^{2+}$ (aq) +$\cdot S_2O_8^-$ (3) $Fe^{2+}$ (aq) + $\cdot SO_4^-$ (aq) $\rightarrow$ $Fe^{2+}$ + $SO_4^{2-}$ (aq) [28]. This was similar to the findings of Zhang et al., who discovered that the highest TPH degradation rate (59.77%) in soil was achieved when PS:FeSO$_4$ = 2:4. However, increasing this ratio resulted in a decrease in the degradation rate, with the most significant decrease (35.51%) occurring when PS:FeSO$_4$ = 2:6 [29].
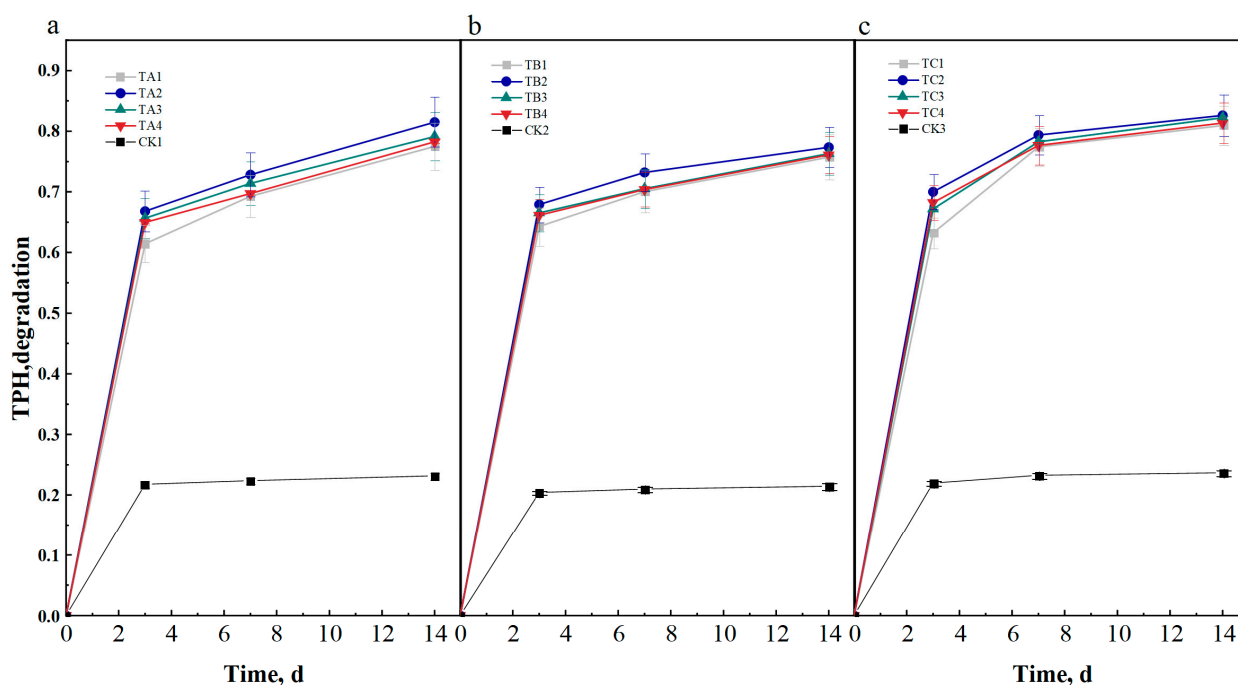


**Figure 7.** Changes in the TPH degradation rate in soil with PS oxidation remediation for 14 d: PS:FeSO$_4$ = 1:0.8 (TA1/TB1/TC1), PS:FeSO$_4$ = 1:1 (TA2/TB2/TC2), PS:FeSO$_4$ = 1:1.2 (TA3/TB3/TC3), PS:FeSO$_4$ = 1:1.4 (TA4/TB4/TC4). (**a**) Experimental conditions: initial TPH concentration = 19,070 ± 477.3 mg/kg, pH = 6.84; (**b**) Experimental conditions: TPHs = 14,792 ± 350.5 mg/kg, pH = 6.62; (**c**) Experimental conditions: TPHs = 10,801 ± 200.9 mg/kg, pH = 6.59.

### 3.3. Changes in the Physicochemical Properties of Soil After Oxidation

The physicochemical properties of soils with varying TPH concentrations, 14 days after oxidation with different PS:FeSO$_4$ ratios, are shown in Table 2. In all treatments, total nitrogen and phosphorus levels were higher than in the control. This may have occurred due to the decomposition of TPHs, which reduced the amount of toxic substances (e.g., PAHs) in the soil, thereby enhancing the activity of nitrogen-fixing and phosphorus-solubilizing microorganisms. However, the organic matter content was lower in the treated soils compared to the control, likely because the FeSO$_4$-activated PS not only degraded TPHs but also oxidized organic matter in the soil [30]. There was also a decrease in soil pH, causing soil acidity and a reduction in the soil's buffering capacity [8,31]. Previous studies have also reported similar results, with high doses of PS reducing the soil's buffering capacity [32,33]. In all PS treatments for TPH-contaminated soils, when PS:FeSO$_4$ = 1:1 and 1:0.8, there were smaller decreases in soil pH, indicating a weaker effect on soil acidification. This suggests that the buffering capacity of the soil was less damaged under this treatment than under the others. This may be because the PS was fully activated with less residual Fe$^{2+}$, which was oxidized to Fe$^{3+}$. After hydrolysis, the acidity of Fe$^{2+}$ is greater than that of Fe$^{3+}$ [34].

**Table 2.** Soil organic matter (SOM), total N, total P, total K, and pH before and after PS oxidation remediation. High-TPH soil (Row 1) experimental conditions: initial TPH concentration = 19,070 ± 477.3 mg/kg, pH = 6.84; medium-TPH soil (Row 2) experimental conditions: initial TPH concentration = 14,792 ± 350.5 mg/kg, pH = 6.62; low-TPH soil (Row 3) experimental conditions: TPHs = 10,801 ± 200.9 mg/kg, pH = 6.70.

| Soil Sample | CK1 | TA1 | TA2 | TA3 | TA4 |
|---|---|---|---|---|---|
| Total N (g/kg) | 95.58 ± 5.3 | 104.7 ± 6.3 | 111.5 ± 5.5 | 109.2 ± 7.1 | 100.1 ± 6.6 |
| Total P (g/kg) | 1.392 ± 0.01 | 1.652 ± 0.01 | 1.948 ± 0.02 | 1.652 ± 0.01 | 1.689 ± 0.015 |
| Total K (g/kg) | 3.23 ± 0.02 | 3.19 ± 0.025 | 3.33 ± 0.012 | 3.01 ± 0.022 | 3.49 ± 0.017 |
| SOM (g/kg) | 30.7 ± 0.3 | 30.6 ± 0.2 | 29.1 ± 0.15 | 28.9 ± 0.2 | 27.5 ± 0.1 |
| pH | 6.84 ± 0.04 | 4.20 ± 0.05 | 4.25 ± 0.08 | 4.07 ± 0.1 | 4.08 ± 0.06 |
| Soil Sample | CK2 | TB1 | TB2 | TB3 | TB4 |
| Total N (g/kg) | 91.12 ± 5.3 | 94.44 ± 5.3 | 107.0 ± 5.8 | 95.58 ± 6.7 | 97. 85 ± 4.2 |
| Total P (g/kg) | 1.389 ± 0.015 | 1.763 ± 0.01 | 1.800 ± 0.02 | 1.763 ± 0.015 | 1.837 ± 0.02 |
| Total K (g/kg) | 3.22 ± 0.015 | 3.14 ± 0.012 | 3.01 ± 0.015 | 3.20 ± 0.020 | 3.12 ± 0.015 |
| SOM (g/kg) | 33.9 ± 0.10 | 31.7 ± 0.20 | 28.9 ± 0.15 | 30.7 ± 0.10 | 29.9 ± 0.15 |
| pH | 6.62 ± 0.03 | 4.14 ± 0.02 | 4.20 ± 0.015 | 4.00 ± 0.025 | 3.92 ± 0.022 |
| Soil Sample | CK3 | TC1 | TC2 | TC3 | TC4 |
| Total N (g/kg) | 85.31 ± 4.6 | 91.03 ± 5.4 | 87.61 ± 3.1 | 92.17 ± 6.5 | 91.03 ± 7.1 |
| Total P (g/kg) | 1.396 ± 0.02 | 1.689 ± 0.02 | 1.652 ± 0.01 | 1.911 ± 0.015 | 1.689 ± 0.02 |
| Total K (g/kg) | 3.21 ± 0.02 | 3.19 ± 0.01 | 3.11 ± 0.015 | 3.05 ± 0.02 | 3.14 ± 0.020 |
| SOM (g/kg) | 32.8 ± 0.3 | 31.3 ± 0.3 | 29.9 ± 0.2 | 29.5 ± 0.15 | 31.3 ± 0.3 |
| pH | 6.59 ± 0.03 | 4.05 ± 0.02 | 4.12 ± 0.01 | 3.89 ± 0.015 | 3.87 ± 0.02 |

The values are the means ± SD. SOM = soil organic matter. PS:FeSO$_4$ = 1:0. 8 (TA1/TB1/TC1), PS:FeSO$_4$ = 1:1 (TA2/TB2/TC2), PS:FeSO$_4$ = 1:1.2 (TA3/TB3/TC3), PS:FeSO$_4$ = 1:1.4 (TA4/TB4/TC4).

### 3.4. Effects of Oxidized Soil on Plant Growth

The effects of different PS:FeSO$_4$ ratios on high-TPH-contaminated soil and crop growth are shown in Figure 8. During the soybean flowering stage, a PS:FeSO$_4$ ratio of 1:1 resulted in a higher net photosynthetic rate, stomatal conductance, and intercellular CO$_2$ concentration than in the other treatments. The transpiration rate was also significantly higher at PS:FeSO$_4$ ratios of 1:0.8 and 1:1. These findings suggest that the TA2 treatment promoted better early growth of soybeans. At the pod-setting stage, the TA2 treatment again produced a significantly higher photosynthetic rate, stomatal conductance, and transpiration rate than the other treatments. This indicates that soybeans grown under the TA2 treatment had slower aging, longer growth cycles, and enhanced dry matter accumulation. However, the intercellular CO$_2$ concentration was lower than in other treatments, likely due to the dense leaf growth, which reduced light intensity and caused partial stomatal closure, limiting gas exchange. Despite this, light intensity remained above the light saturation point, allowing for a higher net photosynthetic rate [35].
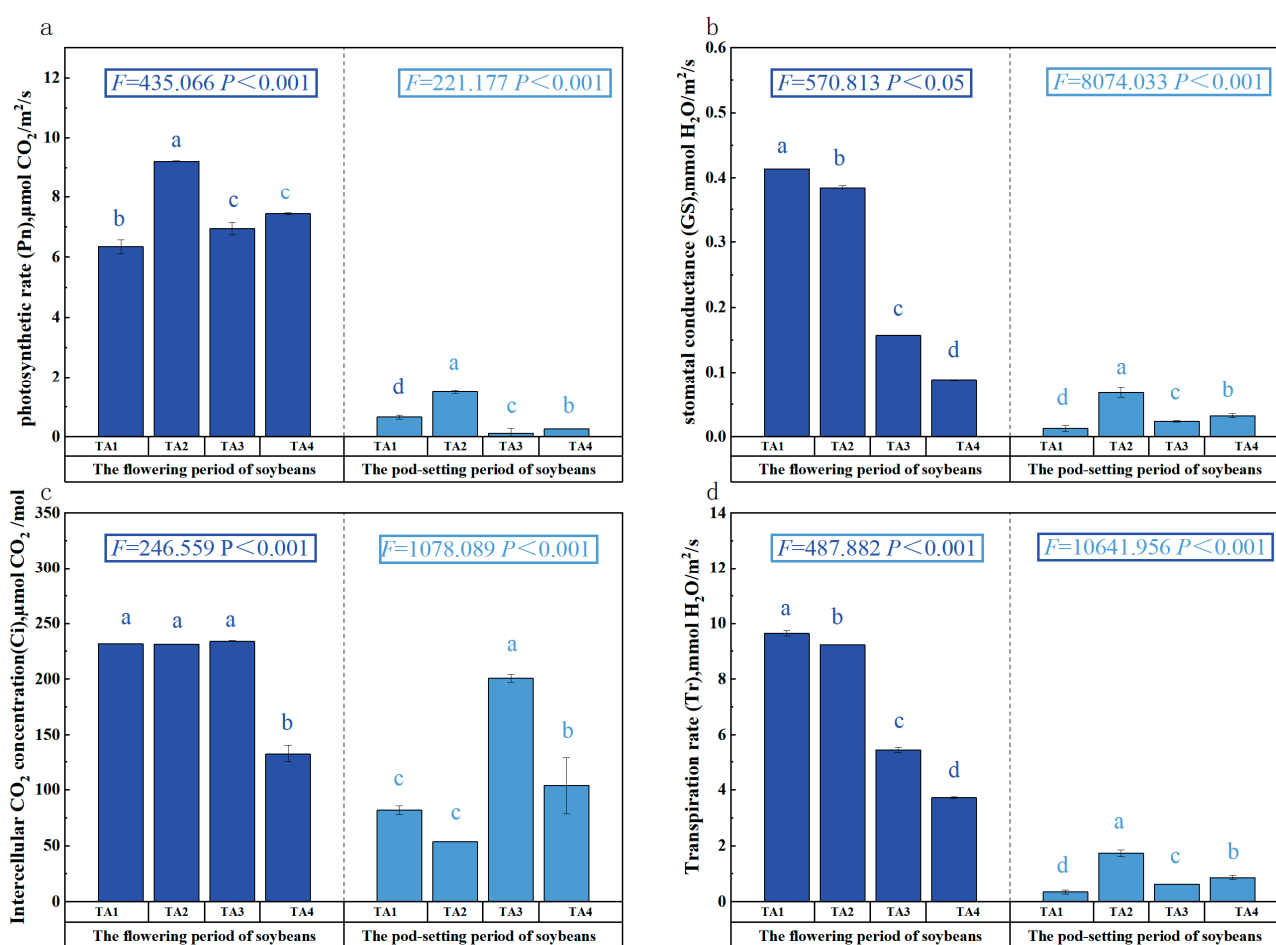


**Figure 8.** The effects of chemical oxidation remediation 14 days after planting soybeans: (**a**) photosynthetic rate; (**b**) stomatal conductance; (**c**) intercellular CO$_2$ concentration; (**d**) transpiration rate. Measurements were made during the flowering and podding stages under the following experimental conditions: initial TPH concentration = 19,070 ± 477.3 mg/kg, pH = 6.84. Different letters (e.g., a, b, c, d) indicate statistically significant differences between groups. The same letter denotes no significant difference, while different letters represent significant differences ($p < 0.001$).

The effects of different PS:FeSO$_4$ ratios on plant growth in medium-TPH-contaminated soil after oxidation are shown in Figure 9. During the soybean flowering stage, the net photosynthetic rate at a PS:FeSO$_4$ ratio of 1:1 was significantly higher than in the other

treatments, while the intercellular $CO_2$ concentration was slightly lower. The stomatal conductance and transpiration rate were notably higher at the $PS:FeSO_4$ ratios of 1:0.8 and 1:1, indicating that soils treated with TB2 and TB3 promoted better early soybean growth. At the pod-setting stage, the TB2 treatment resulted in a significantly higher net photosynthetic rate, stomatal conductance, and transpiration rate compared to other treatments, with both TB2 and TB3 exhibiting superior photosynthetic performance. These findings suggest that soybeans grown under the TB2 and TB3 treatments experienced slower aging, extended growth cycles, and enhanced dry matter accumulation, which could contribute to higher soybean yields. In conclusion, crops grown in soils under the TB2 and TB3 treatments demonstrated the best overall growth performance [36]. This may be because the TB2 and TB3 treatments reduced the degradation of toxic substances such as PAHs in the soil, which in turn reduced the toxicity to soybeans. Wang et al. also reported similar results, with the chlorophyll content, superoxide dismutase activity, and nitrate reductase activity decreasing sharply when the TPH concentration was $8000-10,000$ mg/kg, while the peroxidase activity increased [37,38]. The inhibitory effect gradually strengthened with increasing concentration, causing significant toxicity to soybean seedlings [39].
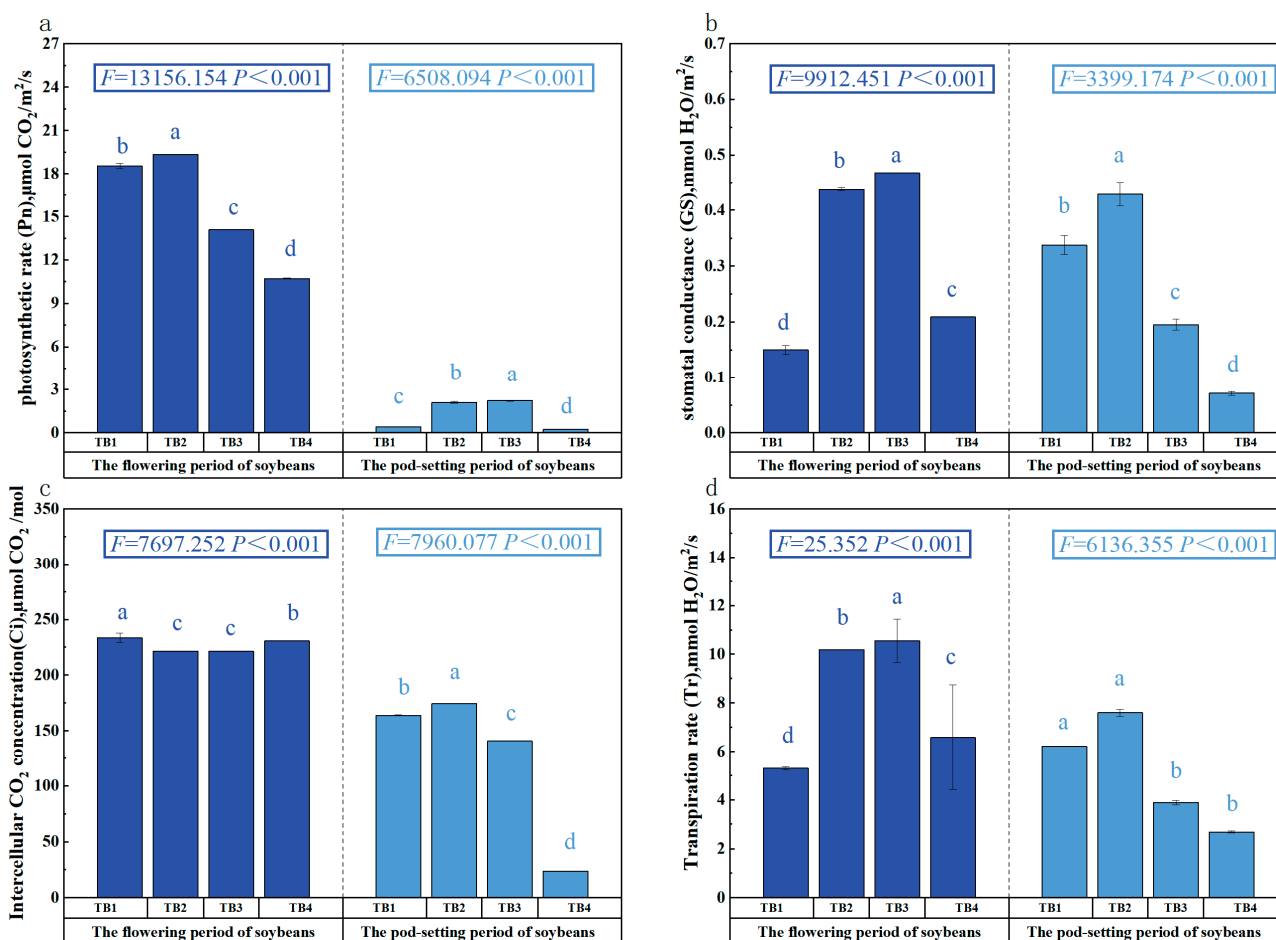


**Figure 9.** The effects of chemical oxidation remediation 14 days after planting soybeans: (**a**) photosynthetic rate; (**b**) stomatal conductance; (**c**) intercellular $CO_2$ concentration; (**d**) transpiration rate. Measurements were made during the flowering and podding stages under the following experimental conditions: initial TPH concentration = $14,792 \pm 350.5$ mg/kg, pH = 6.62. Different letters (e.g., a, b, c, d) indicate statistically significant differences between groups. The same letter denotes no significant difference, while different letters represent significant differences ($p < 0.001$).

The effects of different PS:FeSO$_4$ ratios on plant growth in low-THP soil after oxidation are shown in Figure 10. During the soybean flowering stage, the photosynthetic rate, stomatal conductance, and transpiration rate were significantly higher at the PS:FeSO$_4$ ratios of 1:1 and 1:1.2 compared to other treatments, while the intercellular CO$_2$ concentration was slightly lower. These results suggest that the soils treated with TC2 and TC3 were more conducive to early soybean growth. At the pod-setting stage, TC2 had a significantly higher net photosynthetic rate, stomatal conductance, intercellular CO$_2$ concentration, and transpiration rate than the other treatments [40,41]. This indicates that soybeans grown in TC2-treated soil experienced slower aging, extended growth cycles, and enhanced dry matter accumulation. Overall, crops grown in TC2-treated soils exhibited the best growth performance. Crops exposed to petroleum-contaminated environments exhibit physiological responses such as decreased photosynthetic efficiency, restricted root development, and reduced seed germination rates. The study by Rashid et al. (2023) reached similar conclusions, finding that crops exposed to petroleum-contaminated environments show reduced photosynthetic efficiency, stunted root development, and lower seed germination rates. In soils with higher levels of pollution, the accumulation of these harmful compounds exacerbates, further deteriorating plant health [42–44].
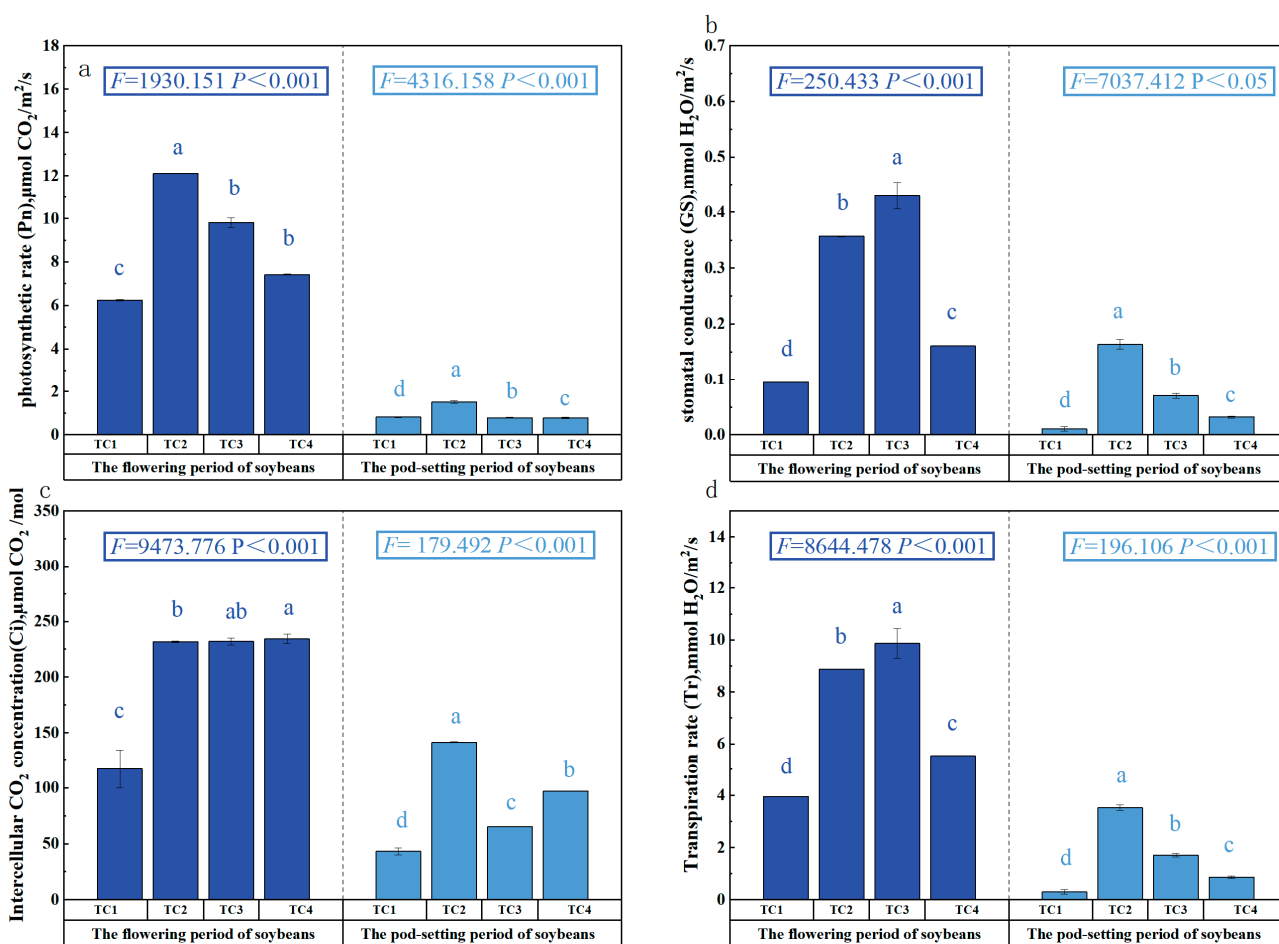


**Figure 10.** The effects of chemical oxidation remediation 14 days after planting soybeans: (**a**) photosynthetic rate; (**b**) stomatal conductance; (**c**) intercellular CO$_2$ concentration; (**d**) transpiration rate. Measurements were made during the flowering and podding stages under the following experimental conditions: initial TPH concentration = 10,801 ± 200.9 mg/kg, pH = 6.70. Different letters (e.g., a, b, c, d) indicate statistically significant differences between groups. The same letter denotes no significant difference, while different letters represent significant differences ($p < 0.001$).

Figure 11 shows a correlation heatmap between the physiological traits during the flowering and podding stages of soybeans. During the flowering stage, the stomatal conductance and transpiration rate exhibited a highly significant positive correlation. This also significantly affected the net photosynthetic rate during the podding stage, which was therefore positively correlated with these parameters. Moreover, the net photosynthetic rate during the soybean flowering stage was significantly and positively correlated with the stomatal conductance, intercellular $CO_2$ concentration, and transpiration rate during the pod-setting stage. This indicates that the growth status of soybeans during the flowering stage significantly and positively affect the growth status during the podding stage. In high-, medium-, and low-TPH soils, compared to the other treatments, when PS:FeSO$_4$ = 1:1, the physiological indicators during the flowering stage were maintained at a higher level, i.e., the growth status was better. Because the growth during the flowering period significantly affected the growth conditions during the pod-setting period, during the soybean podding stage, a better growth status was achieved, and a high photosynthetic rate was maintained. This caused an increase in soybean dry matter accumulation, thereby increasing the soybean yield [45,46]. The study by Yadav, S. K., et al. also reached similar conclusions. High concentrations of petroleum hydrocarbons, particularly in the form of heavy oils or tarry residues, can limit plant growth and microbial activity. This was likely due to the lower TPH concentration in the soil, which reduced root toxicity and supported healthier plant growth [47,48].
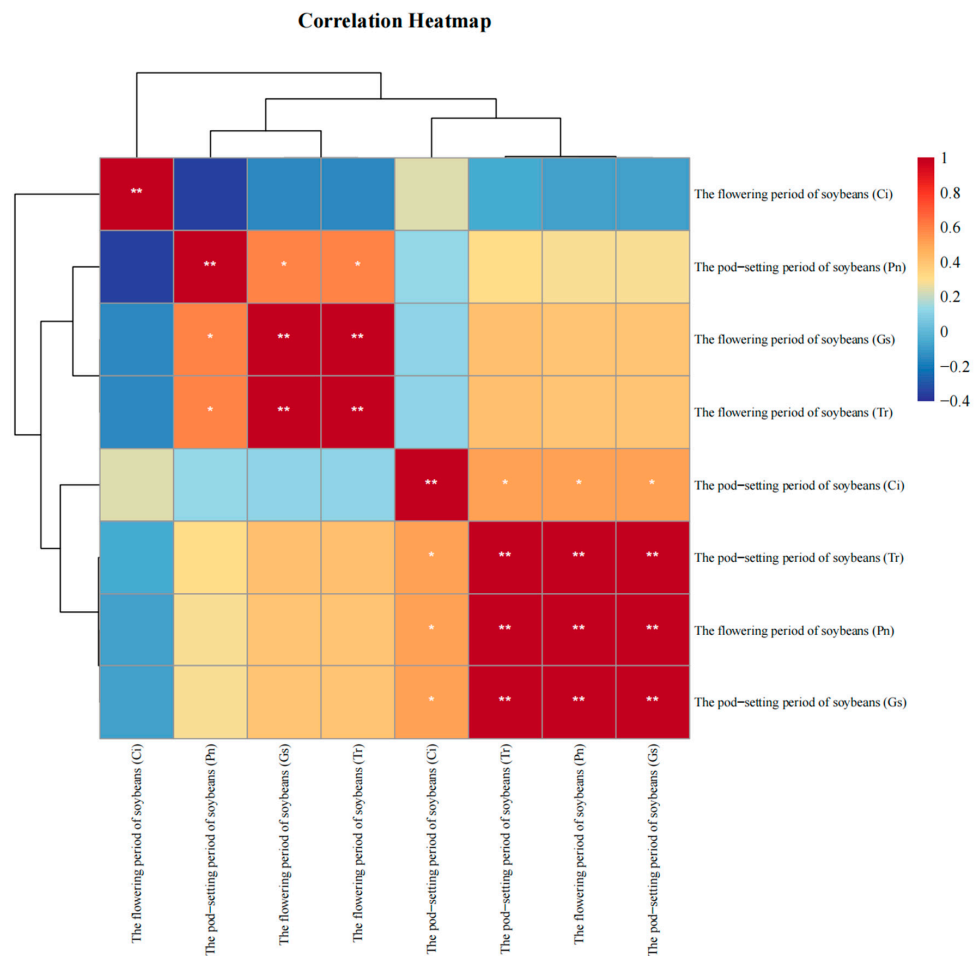


**Figure 11.** Heatmap of the correlation between different PS:FeSO$_4$ ratios in the remediation of soil contaminated with various TPH concentrations and the physiological indicators of soybeans. "*" indicates a significant correlation between factors, while "**" indicates a highly significant correlation between factors.

## 4. Conclusions

In TPH-contaminated soils, after 14 days of chemical oxidation remediation, the TPH degradation rate was highest (81.5%, 81.4%, and 73.5%) for high-, medium-, and low-TPH soils, respectively, when PS:FeSO$_4$ = 1:1. The analysis of the physical and chemical properties after remediation indicated that PS oxidation degraded TPHs and also oxidized organic matter in the soil, leading to soil acidification and a decrease in the soil's buffering capacity. However, when PS:FeSO$_4$ = 1:1, the soil's buffering capacity was less impacted. The verification experiment on soybean cultivation after soil restoration found that, in all treatments, the PS:FeSO$_4$ ratio of 1:1 for high-, medium-, and low-TPH soils had the least impact on soybean growth. The photosynthetic rate, stomatal conductance, intercellular CO$_2$ concentration, and transpiration rate were all higher than under the other treatments. Therefore, a PS:FeSO$_4$ ratio of 1:1 not only reduced the soil TPH concentration, it also had a lesser impact on the original physical and chemical properties and sustainable reuse of the soil than the other treatments.

## Abbreviations

PS—persulfate; ISCO—in situ chemical oxidation; TPHs—total petroleum hydrocarbons; PAHs—polycyclic aromatic hydrocarbons; H$_2$O$_2$—hydrogen peroxide; ($\cdot$SO$_4$)—sulfate radical; UV—ultraviolet light; pH—potential of hydrogen; FeSO$_4$ —ferrous sulfate; Fe$^{2+}$—ferrous ion; Fe$^{3+}$—ferric ion; Na$_2$S$_2$O$_8$—sodium persulfate; CO$_2$—carbon dioxide; SOM—soil organic matter; N—nitrogen; P—phosphorus; K—potassium; Pn—photosynthetic rate; GS—stomatal conductance; Ci—intercellular CO$_2$ concentration; Tr—transpiration rate.

## References

1. Hu, G.; Li, J.; Zeng, G. Recent development in the treatment of oily sludge from petroleum industry: A review. *J Hazard Mater.* **2013**, *261*, 470–490. [CrossRef] [PubMed]
2. Savonina, E.; Maryutina, T. Use of rotating-coiled columns for sample preparation in the analysis of petropolluted soils. *J. Anal. Chem.* **2008**, *63*, 618–621. [CrossRef]
3. Wu, H.; Sun, L.; Wang, H.; Wang, X. Persulfate Oxidation for the Remediation of Petroleum Hydrocarbon-Contaminated Soils. *Pol. J. Environ. Stud.* **2016**, *25*, 851–857. [CrossRef] [PubMed]
4. Zhu, C.; Zhu, F.; Wang, F.; Gao, J.; Fan, G.; Zhou, D.; Fang, G. Comparison of Persulfate Activation and Fenton Reaction in Remediating an Organophosphorus Pesticides-Polluted Soil. *Pedosphere* **2017**, *27*, 465–474. [CrossRef]
5. Lv, Y.; Bao, J.; Zhu, L. A comprehensive review of recent and perspective technologies and challenges for the remediation of oil-contaminated sites. *Energy Rep.* **2022**, *8*, 7976–7988. [CrossRef]
6. Liao, X.; Wu, Z.; Li, Y.; Cao, H.; Su, C. Effect of various chemical oxidation reagents on soil indigenous microbial diversity in remediation of soil contaminated by PAHs. *Chemosphere* **2019**, *226*, 483–491. [CrossRef] [PubMed]

7.    Li, D.; Zhao, Y.; Wang, L.; Wei, S.; Huang, S. Remediation of phenanthrene contaminated soil through persulfate oxidation coupled microbial fortification. *J. Environ. Chem. Eng.* **2021**, *9*, 106098. [CrossRef]

8.    Liu, N.; Wang, L.; Cao, D.; Li, D.; Zhu, Y.; Huang, S.; Shi, J. Remediation of petroleum contaminated soil by persulfate oxidation coupled with microbial degradation. *J. Environ. Chem. Eng.* **2023**, *11*, 109910. [CrossRef]

9.    Duan, X.; Sun, H.; Ao, Z.; Zhou, L.; Wang, G.; Wang, S. Unveiling the active sites of graphene-catalyzed peroxymonosulfate activation. *Carbon* **2016**, *107*, 371–378. [CrossRef]

10.   Duan, X.; Yang, S.; Wacławek, S.; Fang, G.; Xiao, R.; Dionysiou, D.D. Limitations and prospects of sulfate-radical based advanced oxidation processes. *J. Environ. Chem. Eng.* **2020**, *8*, 103849. [CrossRef]

11.   Kaur, B.; Kuntus, L.; Tikker, P.; Kattel, E.; Trapido, M.; Dulova, N. Photo-induced oxidation of ceftriaxone by persulfate in the presence of iron oxides. *Sci. Total. Environ.* **2019**, *676*, 165–175. [CrossRef] [PubMed]

12.   Sutton, N.B.; Grotenhuis, J.T.C.; Langenhoff, A.A.M.; Rijnaarts, H.H.M. Efforts to improve coupled in situ chemical oxidation with bioremediation: A review of optimization strategies. *J. Soils Sed.* **2011**, *11*, 129–140. [CrossRef]

13.   Watts, R.J.; Ahmad, M.; Hohner, A.K.; Teel, A.L. Persulfate activation by glucose for in situ chemical oxidation. *Water Res.* **2018**, *133*, 247–254. [CrossRef] [PubMed]

14.   Fang, G.; Liu, C.; Gao, J.; Dionysiou, D.D.; Zhou, D. Manipulation of persistent free radicals in biochar to activate persulfate for contaminant degradation. *Environ. Sci. Technol.* **2015**, *49*, 5645–5653. [CrossRef]

15.   Jeong, H.-M.; Kim, H.-R.; Hong, S.; You, Y.-H. Effects of elevated CO2 concentration and increased temperature on leaf quality responses of rare and endangered plants. *J. Ecol. Environ.* **2018**, *42*, 1. [CrossRef]

16.   Ding, Z.; Chen, W.; Hou, J.; Wang, Q.; Liu, W.; Christie, P.; Luo, Y. Hydrogen peroxide combined with surfactant leaching and microbial community recovery from oil sludge. *Chemosphere* **2022**, *286*, 131750. [CrossRef] [PubMed]

17.   Xu, J.; Sun, Y.; Tian, G.; Li, X.; Yang, Z. Fast biodegradation of long-alkanes by enhancing bacteria performance rate by per-oxidation. *J. Environ. Manage.* **2022**, *301*, 113933. [CrossRef] [PubMed]

18.   Shah, A.; Wu, X.; Ullah, A.; Fahad, S.; Muhammad, R.; Yan, L.; Jiang, C. Deficiency and toxicity of boron: Alterations in growth, oxidative damage and uptake by citrange orange plants. *Ecotoxicol. Environ. Saf.* **2017**, *145*, 575–582. [CrossRef]

19.   Ekwuluo, M.O.; Udom, G.J.; Osu, C.I.; Ebiana, C.A. Advances on Chemical Oxidants for Remediation of Ground Water Contaminated with Petrolem Hydrocarbon Products. *IOSR J. Environ. Sci. Toxicol. Food Technol.* **2018**, *12*, 76–81.

20.   Gou, Y.; Zhao, Q.; Yang, S.; Wang, H.; Qiao, P.; Song, Y.; Cheng, Y.; Li, P. Removal of polycyclic aromatic hydrocarbons (PAHs) and the response of indigenous bacteria in highly contaminated aged soil after persulfate oxidation. *Ecotoxicol. Environ. Saf.* **2020**, *190*, 110092. [CrossRef] [PubMed]

21.   Li, Y.-T.; Zhang, J.-J.; Li, Y.-H.; Chen, J.-L.; Du, W.-Y. Treatment of soil contaminated with petroleum hydrocarbons using activated persulfate oxidation, ultrasound, and heat: A kinetic and thermodynamic study. *Chem. Eng. J.* **2022**, *428*, 131336. [CrossRef]

22.   Satapanajaru, T.; Chokejaroenrat, C.; Sakulthaew, C.; Yoo-Iam, M. Remediation and Restoration of Petroleum Hydrocarbon Containing Alcohol-Contaminated Soil by Persulfate Oxidation Activated with Soil Minerals. *Water Air Soil Pollut.* **2017**, *228*, 345. [CrossRef]

23.   Gujar, S.K.; Divyapriya, G.; Gogate, P.R.; Nidheesh, P.V. Environmental applications of ultrasound activated persulfate/peroxymonosulfate oxidation process in combination with other activating agents. *Crit. Rev. Environ. Sci. Technol.* **2023**, *53*, 780–802. [CrossRef]

24.   Gharaee, A.; Khosravi-Nikou, M.R.; Anvaripour, B. Hydrocarbon contaminated soil remediation: A comparison between Fenton, sono-Fenton, photo-Fenton and sono-photo-Fenton processes. *J. Ind. Eng. Chem.* **2019**, *79*, 181–193. [CrossRef]

25.   Moradi, M.; Elahinia, A.; Vasseghian, Y.; Dragoi, E.-N.; Omidi, F.; Khaneghah, A.M. A review on pollutants removal by Sono-photo-Fenton processes. *J. Environ. Chem. Eng.* **2020**, *8*, 104330. [CrossRef]

26.   Salimnezhad, A.; Soltani-Jigheh, H.; Soorki, A.A. Effects of oil contamination and bioremediation on geotechnical properties of highly plastic clayey soil. *J. Rock Mech. Geotech. Eng.* **2021**, *13*, 653–670. [CrossRef]

27.   Bajagain, R.; Lee, S.; Jeong, S.-W. Application of persulfate-oxidation foam spraying as a bioremediation pretreatment for diesel oil-contaminated soil. *Chemosphere* **2018**, *207*, 565–572. [CrossRef] [PubMed]

28.   Chen, G.; Yuan, M.; Ma, B.; Ren, Y. Responses of Petroleum Contamination at Different Sites to Soil Physicochemical Properties and Indigenous Microbial Communities. *Water Air Soil Pollut.* **2023**, *234*, 494. [CrossRef]

29.   Zhang, Z.Y.; Jia, H.Z.; Wang, L.J. Experimental study of the repair of $Fe^{2+}$ activated persulfate in oil contaminated soils. *Acta Petrol. Mineral.* **2017**, *36*, 881–886.

30.   Gou, Y.; Zhao, Q.; Yang, S.; Qiao, P.; Cheng, Y.; Song, Y.; Sun, Z.; Zhang, T.; Wang, L.; Liu, Z. Enhanced degradation of polycyclic aromatic hydrocarbons in aged subsurface soil using integrated persulfate oxidation and anoxic biodegradation. *Chem. Eng. J.* **2020**, *394*, 125040. [CrossRef]

31.   Zhang, B.; Guo, Y.; Huo, J.; Xie, H.; Xu, C.; Liang, S. Combining chemical oxidation and bioremediation for petroleum polluted soil remediation by BC-nZVI activated persulfate. *Chem. Eng. J.* **2020**, *382*, 123055. [CrossRef]

32. Gadouri, H.; Harichane, K.; Ghrici, M. Effect of sodium sulphate on the shear strength of clayey soils stabilised with additives. *Arab. J. Geosci.* **2017**, *10*, 218. [CrossRef]

33. Chen, K.-F.; Chang, Y.-C.; Chiou, W.-T. Remediation of diesel-contaminated soil using in situ chemical oxidation (ISCO) and the effects of common oxidants on the indigenous microbial community: A comparison study. *J. Chem. Technol. Biotechnol.* **2016**, *91*, 1877–1888. [CrossRef]

34. Li, Y.-T.; Sui, Q.; Li, X.; Wang, Y.-Q.; Liu, X.-Y.; Liu, H.; Du, W.-Y. Enhanced in-situ zero-valent iron activated persulfate oxidation with electrokinetics for the remediation of petroleum hydrocarbon contaminated soil. *J. Environ. Chem. Eng.* **2024**, *12*, 113781. [CrossRef]

35. Hu, T.; Zeng, H.; Hu, Z.; Qv, X.; Chen, G. Overexpression of the Tomato 13-Lipoxygenase Gene TomloxD Increases Generation of Endogenous Jasmonic Acid and Resistance to Cladosporium fulvum and High Temperature. *Plant. Mol. Biol. Rep.* **2013**, *31*, 1141–1149. [CrossRef]

36. Xia, F.; Li, B.; Song, K.; Wang, Y.; Hou, Z.; Li, H.; Zhang, X.; Li, F.; Yang, L. Polyploid Genome Assembly Provides Insights into Morphological Development and Ascorbic Acid Accumulation of Sauropus androgynus. *Int. J. Mol. Sci.* **2024**, *25*, 300. [CrossRef]

37. Khayat, M.; Rahnama, A.; Lorzadeh, S.; Lack, S. Physiological Indices, Phenological Characteristics and Trait Evaluation of Canola Genotypes Response to Different Planting Dates. *Proc. Natl. Acad. Sci. India Sect. B Biol. Sci.* **2018**, *88*, 153–163. [CrossRef]

38. Barbosa, J.P.R.A.D.; Cruz, A.B.; dos Santos Botelho, A.; Pennacchi, J.P.; Santana, G.F. Crop physiology, the technology and the production gap. *Theor. Exp. Plant Physiol.* **2024**, *36*, 567–582. [CrossRef]

39. Gao, H.; Wu, M.; Liu, H.; Xu, Y.; Liu, Z. Effect of petroleum hydrocarbon pollution levels on the soil microecosystem and ecological function. *Environ. Pollut.* **2022**, *293*, 118511. [CrossRef] [PubMed]

40. Bowden, C.L.; Evanylo, G.K.; Zhang, X.; Ervin, E.H.; Seiler, J.R. Soil Carbon and Physiological Responses of Corn and Soybean to Organic Amendments. *Compost. Sci. Util.* **2013**, *18*, 162–173. [CrossRef]

41. Liu, J.; Li, M.; Chang, J.; Cheng, X.; Wang, L.; Liu, Q.; Gao, X. Physiological Characteristics of Soybean Leaves at Different Growth Stages. *Chin. J. Agrometeorol.* **2022**, *43*, 622–632.

42. Moreira, A.; Moraes, L.A.C.; Moretti, L.G. Yield, Yield Components, Soil Chemical Properties, Plant Physiology, and Phosphorus Use Efficiency in Soybean Genotypes. *Commun. Soil. Sci. Plant. Anal.* **2017**, *48*, 2464–2476. [CrossRef]

43. Zhou, Q.; Li, Y.; Wang, X.; Yan, C.; Ma, C.; Liu, J.; Dong, S. Effects of Different Drought Degrees on Physiological Characteristics and Endogenous Hormones of Soybean. *Plants* **2022**, *11*, 2282. [CrossRef] [PubMed]

44. Jumrani, K.; Bhatia, V.S. Identification of drought tolerant genotypes using physiological traits in soybean. *Physiol. Mol. Biol. Plants* **2019**, *25*, 697–711. [CrossRef] [PubMed]

45. Wilson, S.T.; Lok, B.M.; Flanigen, E.M. Crystalline metallophosphate compositions. U.S. Patent 4,310,440, 12 January 1982.

46. Mulchi, C.; Slaughter, L.; Saleem, M.; Lee, E.; Pausch, R.; Rowland, R. Growth and physiological characteristics of soybean in open-top chambers in response to ozone and increased atmospheric $CO_2$. *Agric. Ecosyst. Environ.* **1992**, *38*, 107–118. [CrossRef]

47. Wang, X.; Wu, Z.; Zhou, Q.; Wang, X.; Song, S.; Dong, S. Physiological Response of Soybean Plants to Water Deficit. *Front. Plant Sci.* **2022**, *12*, 809692. [CrossRef]

48. Jamali, Z.H.; Ali, S.; Qasim, M.; Song, C.; Anwar, M.; Du, J.; Wang, Y. Assessment of molybdenum application on soybean physiological characteristics in maize-soybean intercropping. *Front. Plant Sci.* **2023**, *14*, 1240146. [CrossRef] [PubMed]